Available online at www.sciencedirect.com
SCIENCE DIRECT®
Nonlinear Analysis 63 (2005) e1445–e1454
Nonlinear Analysis
www.elsevier.com/locate/na

A non-conforming computational methodology for modeling coupled problems

E. Aulisa[a], S. Manservisi[b], P. Seshaiyer[b,*,1]

[a]*DIENCA, University of Bologna, Via dei colli 16, Bologna, Italy*
[b]*Department of Mathematics and Statistics, Texas Tech University, Box 41042, Lubbock, TX 79409-1042, USA*

Abstract

A variety of engineering applications that involve coupling different physical phenomena, often require detailed finite element analysis to be carried out over complex domains. Often such analysis may be accomplished by dividing the global domain into several local subdomains over each of which a local model can be analyzed independently. The global solution can then be constructed by suitably piecing together local solutions from these individually modeled subdomains. However, during the assembly, it is often too cumbersome, or even infeasible, to coordinate the meshes over separate subdomains. One must therefore, employ non-conforming techniques to accomplish such modeling. In this paper, we develop a non-conforming computational methodology via the mortar finite element method to solve a coupled problem where we are interested in determining the effects of temperature variations on a given flow or the transfer of heat within the flow. Using this method the solution over different subdomains with different multigrid levels is efficiently computed. Our numerical results clearly suggest that the proposed methodology is robust and stable.

Keywords: Coupled processes; Navier–stokes; Multigrid

1. Introduction

In recent years, there has been increasing interest in studying coupled phenomena arising from industrial applications such as energy conversion processes, energy storage, the design

* Corresponding author. Tel.: +1 806 742 2568; fax: +1 806 742 1112.
E-mail address: padhu@math.ttu.edu (P. Seshaiyer).

[1] Supported in part by the National Science Foundation under Grant DMS 0207327.

0362-546X/$ - see front matter © 2005 Elsevier Ltd. All rights reserved.
doi:10.1016/j.na.2005.01.052

of power plants and cooling towers, and crystal growth from the liquid phase, as well as in natural and environmental applications such as meteorology, oceanography, climatology and many more. A thorough understanding of heat transfer, the temperature field, and the associated flow field is therefore, of crucial importance in such applications.

To study the effects of temperature on a fluid, we analyze a coupled model where the temperature is described by the convection–diffusion equation, $\partial T/\partial t + \vec{u} \cdot \nabla T = \alpha \Delta T + Q$ coupled with the flow given by, $\partial \vec{u}/\partial t - \nu \Delta \vec{u} + (\vec{u} \cdot \nabla)\vec{u} + \nabla p = \vec{f}$ in $\Omega \times (0, T)$. Here α is the thermal diffusivity and ν is the viscocity and the coupled system is solved along with the incompressibility and boundary conditions. The source term $\vec{f}$ in the fluid equation is related to the temperature in the convection–diffusion equation in order to reflect the fact that changes in temperature cause variations in the fluid's density and hence leads to a coupled problem. In such problems, it is common to have regions with different flows with different temperatures. To model this effectively, one may employ non-overlapping domain decomposition techniques for coupling different grid meshes. The mortar approach (see for example [3–5,16] and references therein) is one such non-conforming domain decomposition method that allows the coupling of different subdomains with non-matching grids and discretization techniques within a mathematical framework for a variety of applications (see [8,15] and references therein). The basic idea is to replace the strong continuity condition at the interfaces between the different subdomains by a weaker one and obtain the best approximation error.

In order to enforce this continuity over domains with different subgrids, it is also important to construct efficient iterative solvers for the algebraic linear system that arises [1,7,14]. In this regard, multigrid techniques for mortar finite element methods have also been developed [6,10]. The idea is to guarantee that the iterate is contained in a subspace where the saddle point problem is positive definite. In many cases this approach requires the exact solution of a modified Schur complement system within each smoothing step which may be too expensive in the multigrid algorithm. The purpose of this paper is to introduce a non-conforming computational methodology that employs the multigrid approach to solve a coupled non-isothermal Navier–Stokes system and which can be used in conjunction with multiprocessor architectures.

2. Model problem and its discretization

2.1. Weak formulation

In order to define a weak formulation of the model problem, let us introduce the continuous bilinear forms $a(\nu, \vec{u}, \vec{v}) = 2\sum_{i,j=1}^{n} \int_\Omega \nu(\vec{x}) D_{ij}(\vec{u}) D_{ij}(\vec{v})\, \mathrm{d}\vec{x}$ for all $\vec{u}, \vec{v} \in \mathbf{H}^1(\Omega)$ and $b(\vec{v}, r) = -\int_\Omega r \nabla \cdot \vec{v}\, \mathrm{d}\vec{x}$ for all $r \in L^2_0(\Omega)$ and for all $\vec{v} \in \mathbf{H}^1(\Omega)$. Here ν may be a $L^\infty(\Omega)$ function. The trilinear form $c(\vec{w}; \vec{u}, \vec{v})$is defined by $c(\vec{w}; \vec{u}, \vec{v}) = \sum_{i,j=1}^{2} \int_\Omega w_j (\partial u_i/\partial x_j) v_i\, \mathrm{d}\vec{x}$ for all $\vec{w}, \vec{u}, \vec{v} \in \mathbf{H}^1(\Omega)$. For details concerning the function spaces introduced, the bilinear and trilinear forms and their properties, one may consult [2,9,12,13,17].

Let Ω be an open domain with boundary Γ. One part of the boundary $\Gamma_1 \subset \Gamma$ we prescribe velocity Dirichlet boundary conditions. On another part of the boundary $\Gamma_2 \subset \Gamma$

temperature Dirichlet boundary conditions are prescribed. Let $\vec{f} \in \mathbf{L}^2(\Omega)$ be the body force, $Q \in \mathbf{L}^2(\Omega)$ the heat source, $\vec{g}_{\mathrm{v}} \in \mathbf{H}^{1/2}(\Gamma_1)$ the prescribed imposed velocity over Γ_1 satisfying the compatibility condition and $\vec{g}_{\mathrm{T}} \in \mathbf{H}^{1/2}(\Gamma_1)$ the prescribed imposed temperature over Γ_2. The velocity, pressure, temperature, the stress vector fields and the heat flux $(\vec{u}, p, T, \vec{\tau}, q_n) \in \mathbf{H}^1(\Omega) \times L_0^2(\Omega) \times H^1(\Omega) \times \mathbf{H}^{-1/2}(\Gamma) \times H^{-1/2}(\Gamma)$ satisfies

$$
\begin{aligned}
&\left\langle \frac{\partial \vec{u}}{\partial t}, \vec{v} \right\rangle + a(v, \vec{u}, \vec{v}) + c(\vec{u}; \vec{u}, \vec{v}) + b(\vec{v}, p) + \langle \vec{\tau}, \vec{v} \rangle_{\Gamma} = \langle \vec{f}, \vec{v} \rangle,\\
&b(\vec{u}, r) = 0,\\
&\left\langle \frac{\partial T}{\partial t}, w \right\rangle + a(\alpha, T, w) + c(\vec{u}; T, w) + \langle q_n, w \rangle_{\Gamma} = \langle Q, w \rangle,\\
&\langle \vec{u}, \vec{s} \rangle_{\Gamma_1} = \langle \vec{g}_{\mathrm{v}}, \vec{s} \rangle_{\Gamma_1},\\
&\langle T, s \rangle_{\Gamma_2} = \langle g_{\mathrm{T}}, s \rangle_{\Gamma_2}
\end{aligned}
\tag{1}
$$

for all $(\vec{v}, r, w, \vec{s}, s) \in \mathbf{H}^1(\Omega) \times L_0^2(\Omega) \times H^1(\Omega) \times \mathbf{H}^{-1/2}(\Gamma_1) \times H^{-1/2}(\Gamma_2)$. We note that system (1) must be solved for the stress vector $\vec{\tau} = \partial \vec{u}/\partial \vec{n} + \vec{n}\, p \in \mathbf{H}^{-1/2}(\Gamma)$ and the heat flux $q_n = -\alpha \partial T/\partial \vec{n} \in H^{-1/2}(\Gamma)$ as well. We employ a Boussinesq approximation for $\vec{f} = (1 - \beta(T - T_0))\vec{g}$, where T_0 is the average temperature of the medium, β is the coefficient of thermal expansion and $\vec{g}$ the gravity vector. This approximation allows the flow to be driven solely by a temperature gradient. If a fluid at rest is isothermal, then these driving forces are zero. However, heating produces thermal buoyancy forces.

2.2. Non-conforming decomposition

We now introduce the non-conforming mortar formulation of the model problem. Let the domain Ω be partitioned into m non-overlapping subdomains $\{\Omega^i\}_{i=1}^m$ such that $\partial\Omega^i \cap \partial\Omega^j$ $(i \neq j)$ is either empty, a vertex, or a collection of edges of Ω^i and Ω^j. In the latter case, we denote this interface by Γ^{ij} which consists of individual common edges from the domains Ω^i and Ω^j. Let $\vec{f}$ be in $\mathbf{L}^2(\Omega)$, Q in $L^2(\Omega)$, $\vec{g}_{\mathrm{v}}$ in $\mathbf{H}^{1/2}(\Gamma_1)$, $\vec{g}_{\mathrm{T}}$ in $H^{1/2}(\Gamma_1)$. We assume $\vec{\tau}$ and q_n equal to zero over $\Gamma - \Gamma_1$ namely assuming zero stress tensor and zero heat flux whenever non-Dirichlet boundary conditions are imposed. The velocity, pressure, temperature, stress field and heat flux $(\vec{u}^i, p^i, T^i, \vec{\tau}^{ij}, q_n^{ij}) \in \mathbf{H}^1(\Omega^i) \times L_0^2(\Omega^i) \times H^1(\Omega^i) \times \mathbf{H}^{-1/2}(\Gamma^{ij}) \times H^{-1/2}(\Gamma^{ij})$ must satisfy the non-isothermal Navier–Stokes system

$$
\begin{aligned}
&\left\langle \frac{\partial \vec{u}^i}{\partial t}, \vec{v}^i \right\rangle + a(v, \vec{u}^i, \vec{v}^i) + c(\vec{u}^i; \vec{u}^i, \vec{v}^i) + b(\vec{v}^i, p^i) + \langle \vec{\tau}^{ij}, \vec{v}^i \rangle_{\Gamma^{ij}}\\
&\quad = -\langle \rho \vec{g} \beta (T^i - T_0), \vec{v}^i \rangle,\\
&b(\vec{u}^i, r^i) = 0,\\
&\left\langle \frac{\partial T^i}{\partial t}, w^i \right\rangle + a(\alpha, T^i, w^i) + c(\vec{u}^i; T^i, w^i) + \left\langle q_n^{ij}, w^i \right\rangle_{\Gamma^{ij}} = \langle Q, w^i \rangle,
\end{aligned}
$$

$$\langle \vec{u}^i, \vec{s}^i \rangle_{\Gamma_1} = \langle \vec{g}^i_{\mathrm{v}}, \vec{s}^i \rangle_{\Gamma_1},$$
$$\langle T^i, s^i \rangle_{\Gamma_2} = \langle g^i_{\mathrm{T}}, s^i \rangle_{\Gamma_2},$$
$$\langle K^i \vec{u}^i - K^j \vec{u}^j, \vec{s}^{ij} \rangle_{\Gamma^{ij}} = 0,$$
$$\langle K^i T^i - K^j T^j, s^{ij} \rangle_{\Gamma^{ij}} = 0, \tag{2}$$

for all $\vec{v}^i \in \mathbf{H}^1_{\Gamma_1}(\Omega^i)$, $r^i \in L^2_0(\Omega_i)$, $w^i \in H^1_{\Gamma_1}(\Omega^i)$, $\vec{s}^i \in \mathbf{H}^{-1/2}(\Gamma_1)$, $s^i \in H^{-1/2}(\Gamma_2)$, $\vec{s}^{ij} \in \mathbf{H}^{-1/2}(\Gamma^{ij})$ and $s^{ij} \in H^{-1/2}(\Gamma^{ij})$, for $i = 1, 2, \ldots, m$ where the operator K^i is the projection operator (usually the identity) from the space trace $\gamma_{\Gamma^{ij}} u^i \in H^{1/2}(\Gamma^{ij})$ to itself. We employ the same projection operator for velocity components and for temperature. Note that, if the projection operators K^i reduce to the identity operator for all i then the problem in (2) is clearly equivalent to (1).

2.3. Finite element discretization

Let h be a finite element discretization parameter in each subdomain which tends to zero. We consider partitioning the discretized domain Ω_h in m non-overlapping polygonal subdomains Ω^i_h. Over each subdomain Ω^i_h, we employ independent conforming finite elements (standard Taylor–Hood). By starting at the multigrid coarse level l_0, we subdivide Ω^i_h and consequently Ω_h into triangles or rectangles by unstructured families of meshes T^{i,l_0}_h. At this coarse level l_0, as at the generic multigrid level l, the triangulation over all Ω^i_h are dependent and obey finite element compatibility constraints along the interfaces Γ^{ij}_h. Based on the simple element midpoint refinement different multigrid levels can be built to reach a complete unstructured mesh $T^{i,l}_h$ for finite element over the entire domain Ω_h at the top finest multigrid level n_t. Let the maximum size of the triangulation of the multigrid level l be h_l.

Over every macro domain Ω^i_h the coupled problem can be solved over a different level l_i generating a solution mesh over Ω_h consisting of different meshes. We denote $\Omega^i_{h_{l_i}}$ to be the subdomain i where the solution will be computed at the finest multigrid level l_i. Here, h_{l_i} denotes the maximum size of the triangulation of subdomain Ω^i_h, where the equations are solved. Note that we do not enforce any compatibility across the interface of any two subdomains Ω^i_h and Ω^j_h which are assumed to only share a few nodes, with local solutions being computed over each subdomain at different levels.

The finite element bases for the approximate solution can be obtained in a similar way. Finite element approximation spaces can be generated in the usual way, as a function of the characteristics length h_l over each multigrid level l resulting in different approximation spaces over the solution mesh Ω^i_h. On this mesh, we compute the velocity field $\vec{u}^i_h$ at the level l over $\Omega^i_{h_l}$ and an extended function $\widehat{u}^i_h$ is defined over all Ω_h with the same basis functions and over each level l in a standard and regular way. In some part of the domain the solution will not be computed at the top level but a projection operator from the coarser level can always be used to approximate the solution over the extended domain Ω_h and therefore an approximation to the extended function $\widehat{u}^i_h$ is always available. This extended function

has the same value at the same point node if the node of the coarser mesh is included in the finest mesh and this is always the case if the different levels are generated by successive midpoint refinements.

2.4. Multilevel non-conforming approximation

Let us choose the families of finite-dimensional spaces $\mathbf{X}_{h_l} \subset \mathbf{H}^1(\Omega)$ and $S_{h_l} \subset L^2_0(\Omega)$ and $\mathbf{P}_{h_l} = \mathbf{X}_{h_l}|_{\partial\Omega}$, with suitable approximation properties [11] that will allow us to build a regular conforming approximation over each grid and such that the approximate solution belongs to $\mathbf{X}_{h_l}$. The mortar decomposition problem over the domains Ω^i_h $(i = 1, 2, \ldots, m)$ solved on the level l_i surrounded by the domains Ω^j_h with $j \in I_i$ (I_i is the set of the neighboring regions of i) can be obtained by discretizing (2). In the mortar finite element method $\vec{\tau}^{ij}_h$ and q^{ij}_h can be seen as Lagrange multipliers for the velocity matching equations on Γ^{ij}_h. Given $\vec{f} \in \mathbf{L}^2(\Omega)$, $Q \in L^2(\Omega)$, $\vec{g}_{\mathrm{v}} \in \mathbf{H}^{1/2}(\Gamma)$ and $\vec{g}_{\mathrm{T}} \in H^{1/2}(\Gamma)$ we have to find $(\vec{u}^i_{h_{l_i},n}, p^i_{h_{l_i},n}, T^i_{h_{l_i},n}, \vec{\tau}^{ij}_h, q^{ij}_h) \in \mathbf{X}_{h_{l_i}}(\Omega^i_h) \times S_{h_{l_i}}(\Omega^i_h) \times X_{h_{l_i}}(\Omega^i_h) \times \mathbf{P}_{h_{l_i}}(\Gamma^{ij}_h) \times P_{h_{l_i}}(\Gamma^{ij}_h)$satisfying the non-isothermal Navier–Stokes equations

$$
\begin{aligned}
&\frac{1}{\Delta t}\langle \vec{u}^i_{h_{l_i},n}, \vec{v}^i_{h_{l_i}}\rangle + a(\vec{u}^i_{h_{l_i},n}, \vec{v}^i_{h_{l_i}}) + c(\vec{u}^i_{h_{l_i},n}; \vec{u}^i_{h_{l_i},n}, \vec{v}^i_{h_{l_i}})\\
&\quad + b(\vec{v}^i_{h_{l_i}}, p^i_{h_{l_i},n}) + \langle \vec{\tau}^{ij}_{h,n}, \vec{v}^i_{h_{l_i},n}\rangle_{\Gamma^{ij}_h}\\
&\qquad = \frac{1}{\Delta t}\langle \vec{u}^i_{h_{l_i},n-1}, \vec{v}^i_{h_{l_i}}\rangle - \langle \rho\vec{g}\beta(T^i_{h_{l_i},n} - T_0), \vec{v}^i_{h_{l_i}}\rangle,\\
&b(\vec{u}^i_{h_{l_i},n}, r^i_{h_{l_i}}) = 0,\\
&\frac{1}{\Delta t}\langle T^i_{h_{l_i},n}, w^i_{h_{l_i}}\rangle + a(\alpha_h, T^i_{h_{l_i},n}, \vec{v}^i_{h_{l_i}}) + c(\vec{u}^i_{h_{l_i},n}; T^i_{h_{l_i},n}, w^i_{h_{l_i}}) + \langle q^{ij}_{h,n}, w^i_{h_{l_i},n}\rangle_{\Gamma^{ij}_h}\\
&\quad = \frac{1}{\Delta t}\langle T^i_{h_{l_i},n-1}, w^i_{h_{l_i}}\rangle + \langle Q, w^i_{h_{l_i}}\rangle,\\
&\langle \vec{u}^i_{h_{l_i},n}, \vec{s}^i_{h_{l_i}}\rangle_{\Gamma_{1h}} = \langle \vec{g}^i_{vh_{l_i}}, \vec{s}^i_{h_{l_i}}\rangle_{\Gamma_{1h}},\\
&\langle T^i_{h_{l_i},n}, s^i_{h_{l_i}}\rangle_{\Gamma_{1h}} = \langle \vec{g}^i_{Th_{l_i}}, s^i_{h_{l_i}}\rangle_{\Gamma_{1h}},\\
&\langle P_{l_i,l_k}(\vec{u}^i_{h_{l_i}}) - P_{l_j,l_k}(\vec{u}^j_{h_{l_i}}), \vec{s}^{ij}_{h_{l_k}}\rangle_{\Gamma^{ij}_h} = 0,\\
&\langle P_{l_i,l_k}(T^i_{h_{l_i}}) - P_{l_j,l_k}(T^j_{h_{l_i}}), s^{ij}_{h_{l_k}}\rangle_{\Gamma^{ij}_h} = 0,
\end{aligned}
\tag{3}
$$

for $\vec{v}^i_{h_{l_i}} \in \mathbf{X}_{\Gamma_{1h}} \cap \mathbf{H}^1_{\Gamma_1}(\Omega^i_h)$, $r^i_{h_{l_i}} \in S_h(\Omega^i_h)$, $w^i_{h_{l_i}} \in X_{\Gamma_{1h}} \cap H^1_{\Gamma_1}(\Omega^i_h)$, $\vec{s}^i_{h_{l_i}} \in \mathbf{P}_{h_{l_k}}(\Gamma_{1h} \cap \Omega^i_h)$ $s^i_{h_{l_i}} \in P_{h_{l_k}}(\Gamma_{1h} \cap \Omega^i_h)$, $\vec{s}^{ij}_{h_{l_k}} \in \mathbf{P}_{h_{l_k}}(\Gamma^{ij}_h)$, and $s^{ij}_{h_{l_k}} \in P_{h_{l_k}}(\Gamma^{ij}_h)$, for $n = 1, 2, \ldots, N$ and $i = 1, 2, \ldots, m$ where $j \in I_i$ and$l_k = \max\{l_i, l_j\}$ over the multigrid levels available at

the boundary Γ_h^{ij}. In order to assure the greatest accuracy the projection operator $P_{l_i,l_k}(\vec{u})$ projects the velocity from the level l_i to the level l_k which is the finest grid present on the boundary Γ_h^{ij}. With this hypotheses also the Lagrange multipliers $\vec{\tau}_h^{ij}$, q_h^{ij} can be discretized and computed on the finest grid available on Γ_h^{ij}. Since the mesh on the multigrid are unstructured and quite openly constructed the mesh between the domain Ω_h^i and the neighboring domain Ω_h^i can be quite different. Very fine meshes on the region of interest and coarse meshes can be handled with little effort.

We solve system (3) by computing simultaneously the solution for both pressure and velocity. An iterative coupled solution of the linearized and discretized incompressible Navier–Stokes equations requires the approximate solution of sparse saddle point problems. We employ a Vanka-like [18] relaxation operator for the multigrid solution with the mortar finite element formulation for solving the coupled model problem.

3. Computational experiments

In this section, we demonstrate the performance of the non-conforming computational methodology that has been developed to solve the coupled non-isothermal Navier–Stokes model problem. By using this computational technique we will show that, it is possible to explore geometry with different meshes and obtain fast and accurate solutions.

In Fig. 1 on the left, a three-channel geometry is shown which we use for numerical computations. As one can see in Fig. 1 the fluid domain Ω_h is divided into five regions. The top and the bottom regions, denoted by Ω_1 and Ω_2 respectively, are large areas of fluid. These two regions are connected through three narrow channels Ω_3, Ω_4 and Ω_5. The domain Ω_h is insulated but different temperature profiles are maintained along the channels. The boundary Γ_h consists of three rectangular perimeters. The vertical boundary along the first channel is denoted by Γ_1 on the left and Γ_2 on the right. The vertical boundary along the second channel is denoted by Γ_3 on the left and Γ_4 on the right. Finally, the vertical boundary

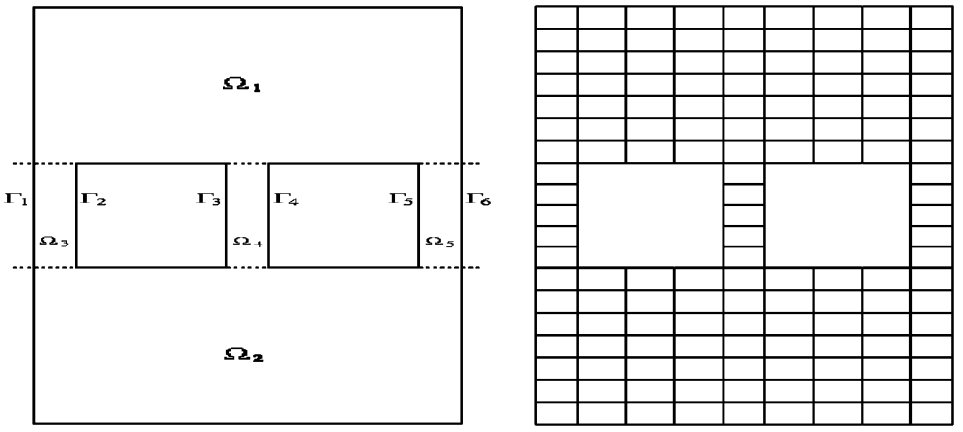

Fig. 1. Computational domain on the left and a regular mesh over level l_0 on the right.

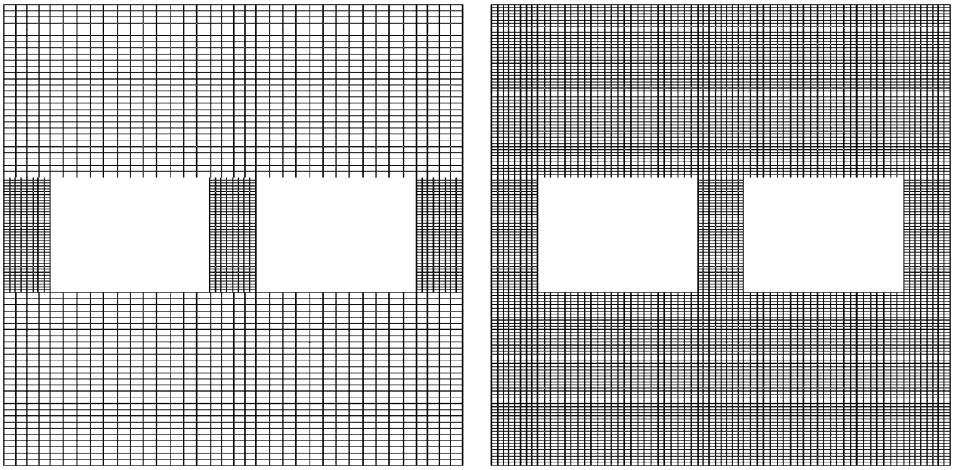

Fig. 2. Mesh over coupled levels $l_3 - l_2$ (case B) on the left and mesh at level l_3 (case A) on the right.

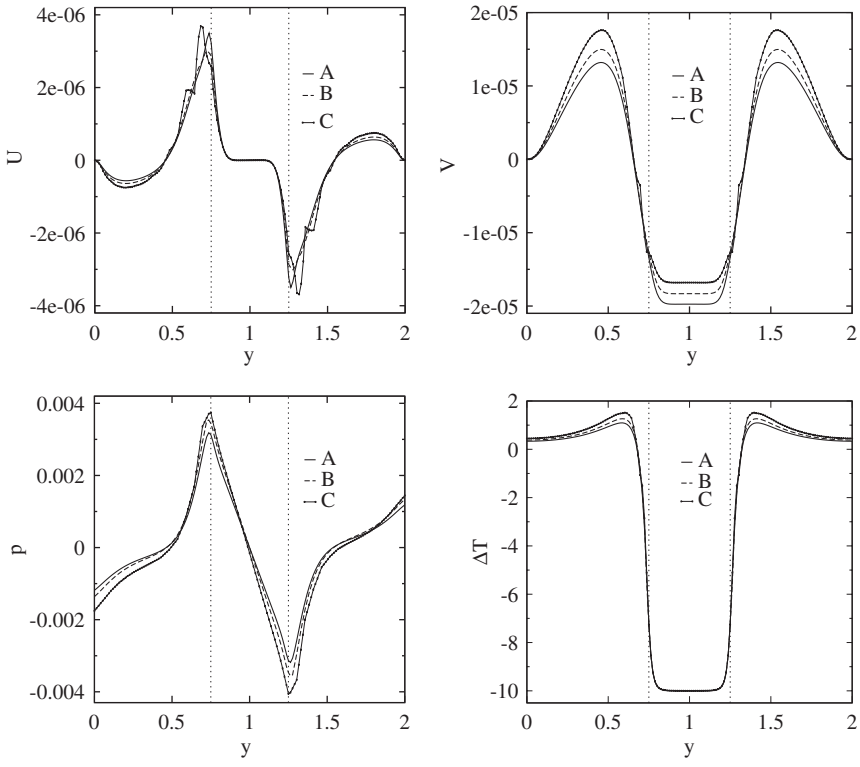

Fig. 3. U and V components of the velocity field, dynamic pressure P and variation in the temperature ΔT, along the y-coordinate at 0.025 m from the left side for different mortar cases A–C.

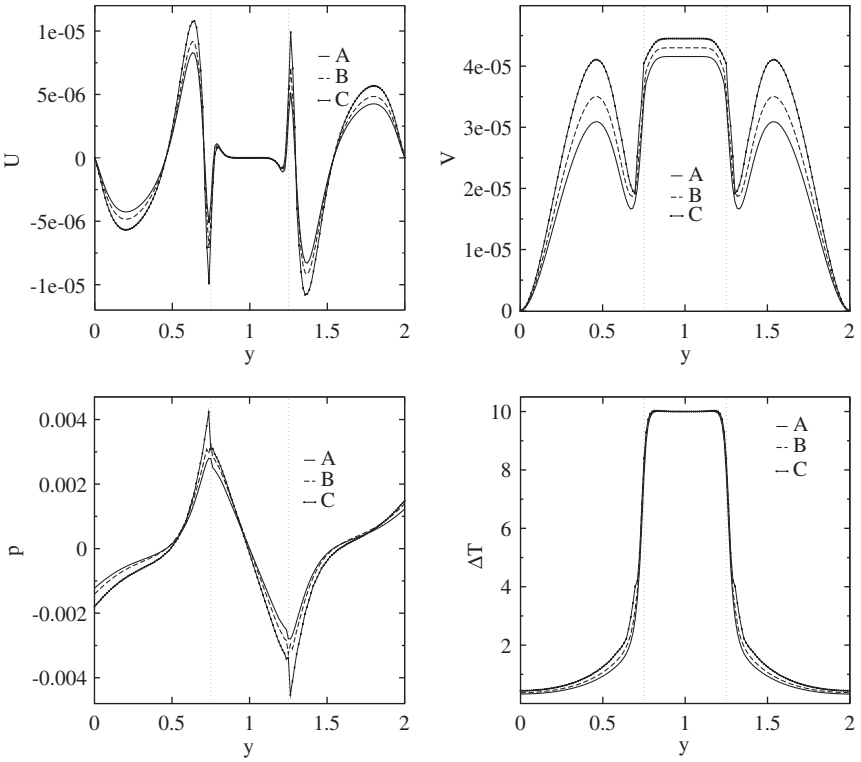

Fig. 4. U and V components of the velocity field, dynamic pressure P and variation in the temperature ΔT, along the y-coordinate at 0.075 m from the left side for different mortar cases A–C.

along the third channel Ω_5 is denoted by Γ_5 on the left and Γ_6 on the right as shown in Fig. 1. In Fig. 1 on the right, the grid at the level l_0 is illustrated. The first multigrid level l_0 is the coarse mesh designed to contain all the relevant information such as boundary conditions and geometric details. The mesh is an unstructured coarse mesh of isoparametric rectangular finite elements with quadratic polynomial for temperature and velocity representation. The other levels l_i $(i = 1, 2, 3)$ are generated by an unstructured grid generator by midpoint refinements. The computations in the regions Ω_h^i $(i = 3, 4, 5)$ should be accurate in order to capture the temperature gradients and the flow motion and therefore solved on the finest grid l_3. In Fig. 2 some possible non-conforming decompositions are illustrated, when the mesh level l_3 over the channels is coupled with different mesh levels over Ω_h^1 and Ω_h^2. In Fig. 2 on the right the uniform mesh is shown over at level l_3. This configuration is the reference configuration and it is defined as case A. In Fig. 2 on the left (case B) the mesh at the level l_3 over Ω_h^i $(i = 3, 4, 5)$ is coupled with level l_2 over Ω_h^1 and Ω_h^2. In the case C, we consider the coupled level $l_3 - l_1$. The boundary conditions for this problem are homogeneous Dirichlet boundary conditions for the velocity and known profiles of temperature along the boundary Γ_i, $i = 1, \ldots, 6$.

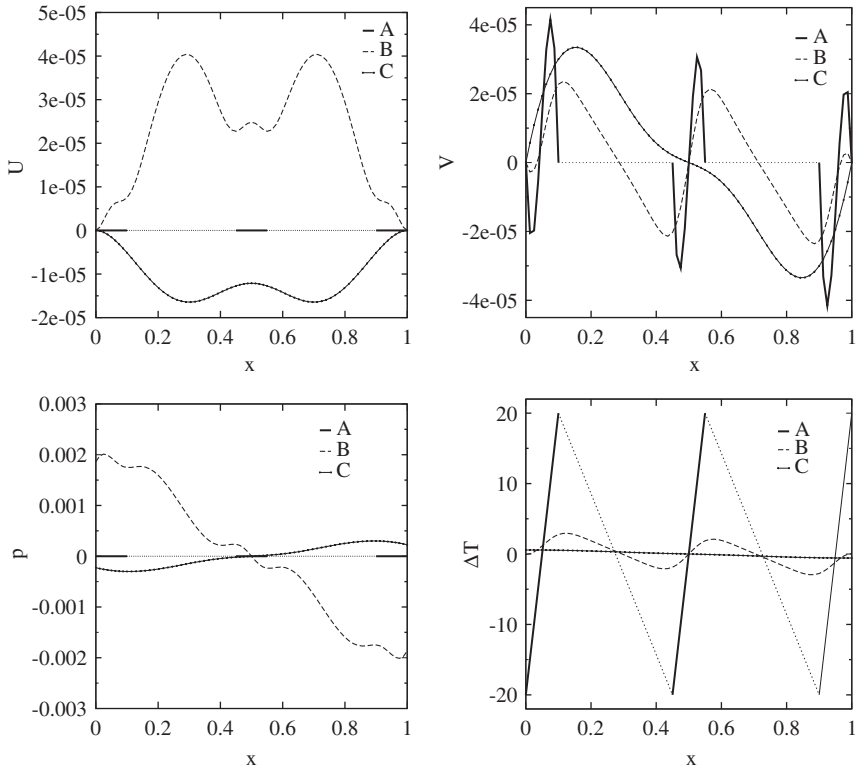

Fig. 5. U and V components of the velocity field, dynamic pressure P and variation in the temperature ΔT, along the x-coordinate at 0.33 m (case C), 0.66 m (case B) and 1 m (case A) from the bottom side of the region Ω_h.

Homogeneous Neumann boundary conditions are applied in the rest of the boundary for the temperature.

As explained previously, one can use the information from the coarse grid to impose boundary conditions on the domains Ω_h^3, Ω_h^4 and Ω_h^5. The procedure computes the Lagrange multipliers $\vec{\tau}_h^{ij}$, q_h^{ij}, the boundary stresses and the surface heat fluxes, implicitly. In this case the solution $\vec{u}_{h_{l_i}}$ and $T_{h_{l_i}}$ is projected by the standard finite element projection operator (the same of the standard multigrid) over the finest grid at level l_3 obtaining the extended solution for $\widehat{u}_h$ and $\widehat{T}_h$ over Ω_h^1 and Ω_h^2. The extended solution generates the boundary conditions for the computation of the solution on the finest grid, which is the union of all Ω_h^i for $i = 3, 4, 5$. The velocity and the temperature on the mesh interfaces are computed iteratively in full agreement with the multigrid approach.

In Figs. 3 and 4 the pressure, the velocity and the temperature solutions $\widehat{p}_h$, $\widehat{u}_h$, $\widehat{T}_h$ along the y-coordinate are plotted for different distances from the left side of the channel Ω_3. Note that the pressure plotted corresponds to the dynamic pressure. Figs. 3 and 4 show the distributions at 0.025 and 0.075 m, respectively, for the different mortar configurations in the cases A–C. The force that drives the motion is the gradient of temperature between the

two sides of the channels which is of 40 °C. A good resolution for the velocity, pressure and temperature requires a mesh at level l_3 in the channel. The solution of the mortar problem in case B is good for both velocity and temperature. The mortar configuration in case C gives reliable temperature distributions while the flow computations must be improved in some regions. In Fig. 5 the velocity field, dynamic pressure and temperature along the x-coordinate at 0.33 m (case A), 0.66 m (case B) and 1 m (case C) from the bottom side of the region Ω_h^1 is shown. All these computations are performed with the mortar configuration corresponding to case B. Oscillations in velocity, pressure, and temperature due to the convective flow are captured and it can be considered satisfactory. The fact that different grids can be used in the narrow channels with respect to the large domain enhances the possibility of reproducing flows in region with different order of magnitude by using reasonable mesh grids.

References

[1] Y. Achdou, Y. Maday, O. Pironneau, Substructuring preconditioners for Q_1 mortar element method, Numer. Math. 71 (1995) 419–449.
[2] R. Adams, Sobolev Spaces, Academic Press, New York, 1975.
[3] F. Ben Belgacem, The mortar finite element method with Lagrange multipliers, Numer. Math. 84 (1999) 173–197.
[4] F. Ben Belgacem, P. Seshaiyer, M. Suri, Optimal convergence rates of *hp* mortar finite element methods for second-order elliptic problems, RAIRO Math. Model. Numer. Anal. 34 (2000) 591–608.
[5] C. Bernardi, Y. Maday, A.T. Patera, Domain decomposition by the mortar element method, in: Asymptotic and Numerical Methods for PDEs with Critical Parameters NATO Adv. Sci. Inst. Ser. C Math. Phys. Sci., Vol. 384, Kluwer Acad. Publ., Dordrecht, 1993, pp. 269–286.
[6] D. Braess, W. Dahmen, C. Wieners, A Multigrid algorithm for the mortar finite element method, SIAM Numer. Anal. 37 (1999) 48–69.
[7] M. Casarin, O. Widlund, A hierarchical preconditioner for the mortar finite element method, ETNA 4 (1996) 75–88.
[8] L.K. Chilton, P. Seshaiyer, The *hp* mortar domain decomposition method for problems in fluid mechanics, Int. J. Numer. Meth. Fluids 40 (2002) 1561–1570.
[9] V. Girault, P. Raviart, The Finite Element Method for Navier–Stokes Equations: Theory and Algorithms, Springer, New York, 1986.
[10] J. Gopalakrishnan, J.E. Pasciak, Multigrid for the mortar finite element method, SIAM Numer. Anal. 37 (2000) 1029–1052.
[11] M. Gunzburger, S. Manservisi, The velocity tracking problem for Navier–Stokes flows with bounded distributed control, SIAM J. Control Optim. 37 (1999) 1913–1945.
[12] M. Gunzburger, S. Manservisi, Analysis and approximation of the velocity tracking problem for Navier–Stokes equations with distributed control, SIAM J. Numer. Anal. 37 (2000) 1481–1512.
[13] M. Gunzburger, S. Manservisi, On a shape control problem for the stationary Navier–Stokes equations, Math. Model. Numer. Anal. 34 (2000) 1233–1258.
[14] R.H.W. Hoppe, Y. Iliash, Y. Kuznetsov, Y. Vassilevski, B. Wohlmuth, Analysis and parallel implementation of adaptive mortar finite element methods, East-West J. Numer. Math. 6 (1998) 223–248.
[15] P. Seshaiyer, Stability and convergence of nonconforming *hp* finite-element methods, Comput. Math. Appl. 46 (2003) 165–182.
[16] P. Seshaiyer, M. Suri, Uniform *hp* convergence results for the mortar finite element method, Math. Comput. 69 (2000) 521–546.
[17] R. Temam, Navier–Stokes Equation, North-Holland, Amsterdam, 1979.
[18] S. Vanka, Block-implicit multigrid calculation of two-dimensional recirculation flows, Comput. Meth. Appl. Mech. Eng. 59 (1986) 29–48.